

Updating Numerical Simulation Model of Sibayak Field, Indonesia

Eric Firanda, Shanti Lasminingsih, Fasya Mediati H., Maulana Fatwa, M. Permadi Sugiharto., M. Bayu Saputra, M. Tajul Arifin, Pudyo Hastuti, Fernando Pasaribu

PT. Pertamina Geothermal Energy Tbk, Grha Pertamina, Medan Merdeka Timur no 11-13, Jakarta, 10110, Indonesia

eric.firanda@pertamina.com

Keywords: Conceptual Model, Numerical Simulation, Natural State

ABSTRACT

The Sibayak Geothermal field is a volcanic geothermal system with the presence of manifestations, located in North Sumatera, Indonesia and is within the Singkut Caldera. Sibayak field is classified into a hot, liquid-dominated geothermal system with temperatures ranging from 240°C to 300°C and an average pressure of 100 barg. The previous numerical model created was in 2001 with data of all 10 wells. However, well data used in this model were solely based on drilling data as field has not been produced. Hence, a newly updated numerical model was made based on the most recent conceptual model as well as reservoir data after the field has started producing in 2008. The natural state of the model was validated by updating well data, whilst calibration of the natural state between simulated and observed data were done by using the most recently obtained pressure-temperature data.

1. INTRODUCTION

The Sibayak Geothermal field is located in Berastagi, Karo Regency, North Sumatera, Indonesia. It is situated in the relatively young Sibayak Mountain, within the Singkut Caldera and has an average elevation of 1400 masl (Figure 1). Preliminary studies were first carried out in 1989 until 1991, which resulted in Mt. Sibayak being a potential field to develop. Three exploratory wells were then drilled in 1991 and were proceeded by drilling 7 development wells by 1997. Partial to total loss circulations were experienced in all of the wells within the field as all wells were successfully drilled through pre-tertiary sedimentary rocks.

Sibayak Geothermal Field started operating in 2008 with a production of 10 MW. The previous numerical model was made in 2001 based on limited drilling and exploration data. More recent geological field surveys as well as magnetotelluric and gravity surveys have been carried out to support the updating of the conceptual model. This updated conceptual model along with a more refined natural state model is thus able to give a more accurate and comprehensive understanding of the reservoir's current condition to further be able to predict the potential reservoir deliverability.

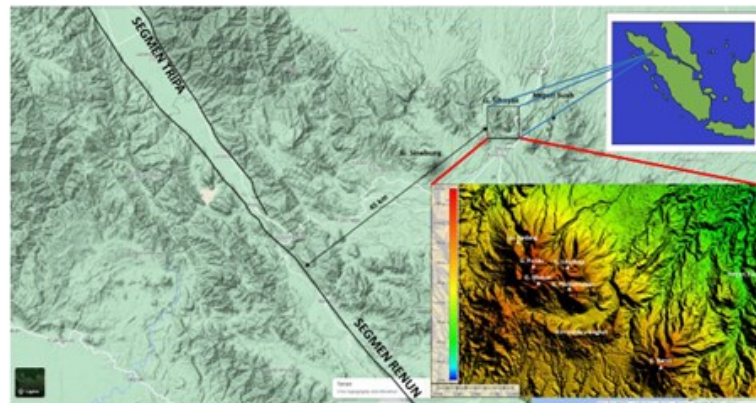


Figure 1: Location of the Sibayak Field.

2. CONCEPTUAL MODEL UPDATE

The geothermal system developed within the Sibayak Geothermal Field is a volcanic-hosted system on the Sibayak Mountain (Figure 2). It involves a high-standing, convective, and high temperature reservoir beneath the summit region of a volcano, in which the geothermal reservoir occurs near the conduit(s) of two small strato-volcanoes in a partly infilled, small caldera (Hochstein et al., 2015).

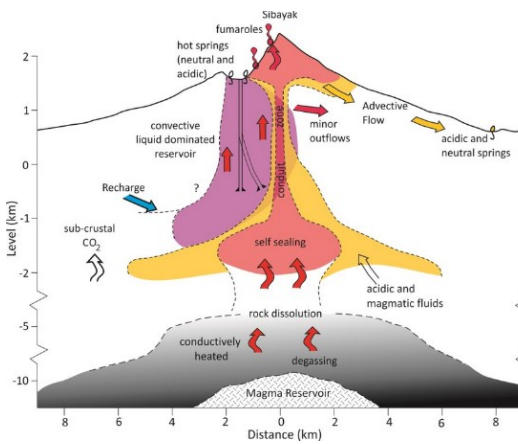


Figure 2: A volcanic-hosted system model (Hochstein et al., 2015).

The presence of various, complex manifestations within the Singkut Caldera and the intensive, altered zone restricted to Mount Sibayak indicate the upflow zone being within and directly under the mountain (Figure 3). This is also supported by recent geochemical analysis of several manifestation samples in which fluid from these manifestations indicate a dominance in volatile magmatic contributions in contrast to meteoric fluids.

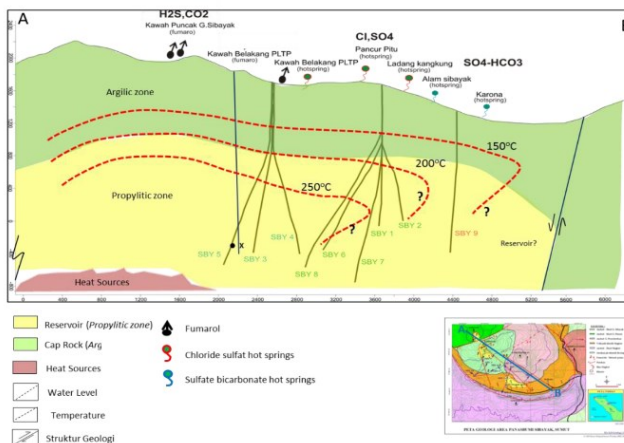


Figure 3: Conceptual model of Sibayak geothermal system (PGE, 2022).

Magnetotelluric (MT) studies have also indicate low resistivities of altered hydrothermal clay cap of 700-1000 m thick indicating the presence of a heat source updoming beneath Mount Sibayak. Based on the magnetotelluric data, the outflow of the hydrothermal system stretches about 3 km E-SE (Figure 4).

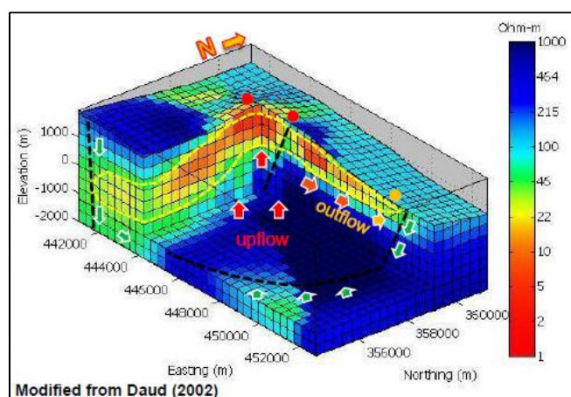


Figure 4: Magnetotelluric (MT) model of Sibayak (modified from Daud, 2001).

Local structures within Sibayak Geothermal Field have an orientation of NW-SE and NE-SW. Apart from extensive fractures, three main faults play a major role as a conduit for hydrothermal activity as well as secondary permeability, namely the Tengkorak Fault, Semangat Gunung Fault, and the Pariban Fault. A ring fault is also present within the Singkut Caldera, hence also contributing to secondary permeability and the flow of hydrothermal activity. The ring fault also acts as the main recharge zone for the geothermal system (Figure 5). Contrary to the isotherms determined in the previous conceptual model, the isotherms of the updated model has considered the recharge flow into the reservoir as well as the length of the outflow zone. Hence, the newly updated conceptual model is able to describe the behavior and characteristics of the reservoir more accurately.

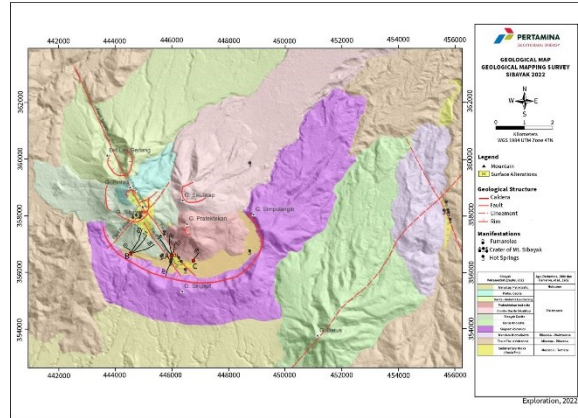


Figure 5: Geological map and stratigraphy of Sibayak (PGE, 2022).

Lithology found within the Sibayak Geothermal Field are pyroxene andesite, dacite, diorite, pyroclastic breccia, volcaniclastic tuff-lapilli as well as Tertiary to Pre-Tertiary metasediments in the form of fine-grained sandstone and silt (Figure 6). As a geothermal system developing within the caldera, volcanic activity within this area plays a major role in the primary permeability resulting in lateral permeability controlled by the volcaniclastic lithology. Main reservoir is within the metasedimentary sandstone, signified by epidotes found as well as total loss to partial loss during the drilling of wells. The presence of faults and fractures within the field also contribute in enhancing the secondary permeability within the field.

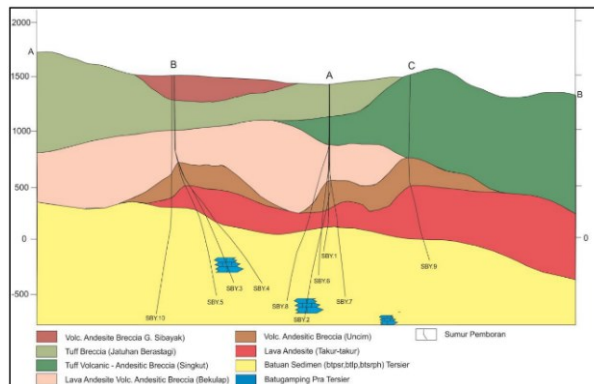


Figure 6: A geologic cross section of Sibayak (PGE, 2016).

3. WELL DATA

Ten wells were drilled from 1992 until 1997 in Sibayak Geothermal Field. SBY-01, SBY-02, and SBY-03 are exploration wells targeting deep, high temperatures and pressures. Epidotes were only identified in two wells, SBY-01 and SBY-03, below the depth of 1156 and 1260 masl, respectively.

Based on the gradual increase of temperature seen in the static temperature and pressure profile indicates a conductive heat transfer process due to low to very low permeability in the formation and existence of the cap rock (Figure 7). This is confirmed with altered andesite cuttings with low permeability retrieved from this depth.

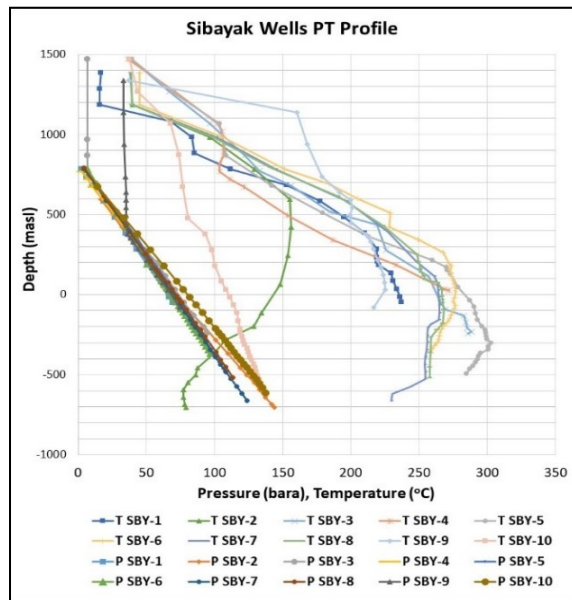


Figure 7: Pressure-temperature profiles of each well in Sibayak Field.

High, consistent temperatures with a relatively convective pattern indicating the presence of the reservoir were found in wells SBY-03, SBY-04, SBY-05, SBY-06, SBY-07 and SBY-08 with maximum temperatures of these wells ranging from 265°C to 302.6°C. These consistent high temperatures most likely reflect the upflow of the system located beneath the Singkut Caldera. High temperatures ranging up to 156°C - 225.5°C were also encountered in wells SBY-01, SBY-02, and SBY-09 but quickly deflected with depth, indicating wells being located on the periphery of the upflow zone and just at edge of the reservoir. The inverse temperatures within these wells also indicate cooler waters flowing in, thus showing the recharge area for the system. SBY-10 had the lowest temperature out of all the wells with a maximum temperature of 124°C and encountered some issues during drilling. Due to the location and elevation of SBY-01, SBY-02, SBY-09 and SBY-10 within the geothermal system, these wells are most suitable to be used as injection wells.

Pressures are relatively high in each of the wells, with maximum pressures found in wells SBY-07 at 125.97 bara. Hydrostatic pressure from ground to total depth of well is clearly visible in the pressure analysis, confirming the reservoir being a hot liquid dominated reservoir. SBY-2 & SBY-10 have a different hydrostatic gradient compared to the other wells, thus confirming the pressure of wells are influenced by well temperatures.

The depth of feedzones were supported by the presence of partial and total loss circulations experienced during the drilling of wells. Feedzones were mostly at depth of -74 masl to -280 masl in a majority of the wells, although feedzones in SBY-5 were found starting from a depth of -405 masl to -425 masl. Feedzones are thought to be controlled by main local fractures and faults in the field, as well as primary permeability control of the metasediments (Figure 8). Injectivity index was highest in SBY-5 at 18.6 kg/s.bar as well as in SBY-6 at 15.4 kg/s.bar. Consequently, the highest mass flow productions were found in well SBY-5 with a contribution of 173 tph of brine and 35 tph of steam.

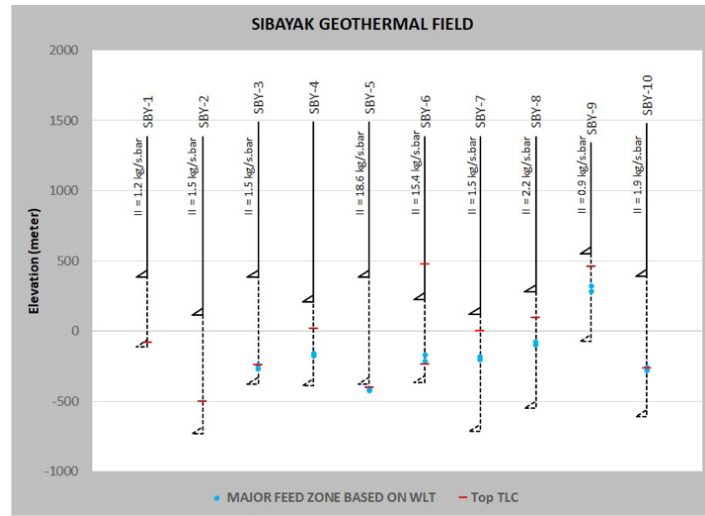


Figure 8: Distribution of feedzones in the wells of Sibayak based on the water loss tests as well as injectivity rates.

4. NUMERICAL MODEL

The Sibayak model was generated using a TOUGH-2 based software by using the first Equation of State module (EOS1). EOS1 assumes the fluids contained within the system is pure water. The model has a dimension of 7.5 km x 8 km with a total area of 60 km² and has an orientation of NW-SE, rotated 34° clockwise (Figure 9).

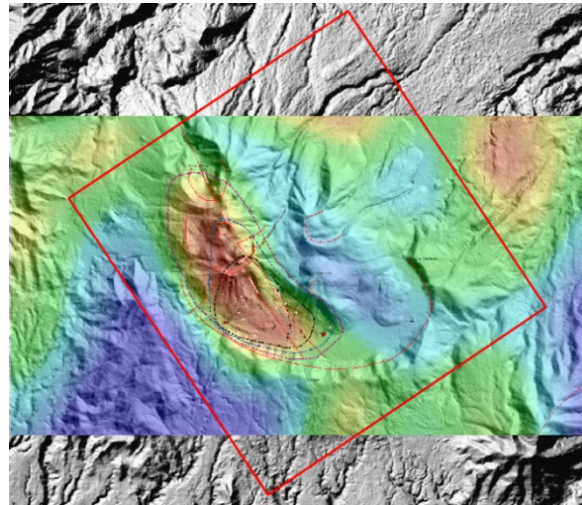


Figure 9: Dimension and orientation of the Sibayak model.

The x-axis was divided into 35 cells, whereas the y-axis was into 38 (Figure 10). Topography of the Sibayak field was considered whilst generating the model with a maximum elevation of +2100 masl and a depth of -2000 masl. The model has 20 layers which are then divided into 5 different properties for the atmosphere, groundwater, caprock, reservoir, and basement. The dimension and size of each cell within the grid varies from 100 – 800 m, depending on the area of interest as well as data availability. Total cells within the model totals up to 26,600 cells with additional extra cells at the base of the model. This new model is thus more detailed and refined compared to the previous model (Atmojo et al., 2001), which was divided into 165 cells laterally and 7 layers totaling up to 1155 cells.

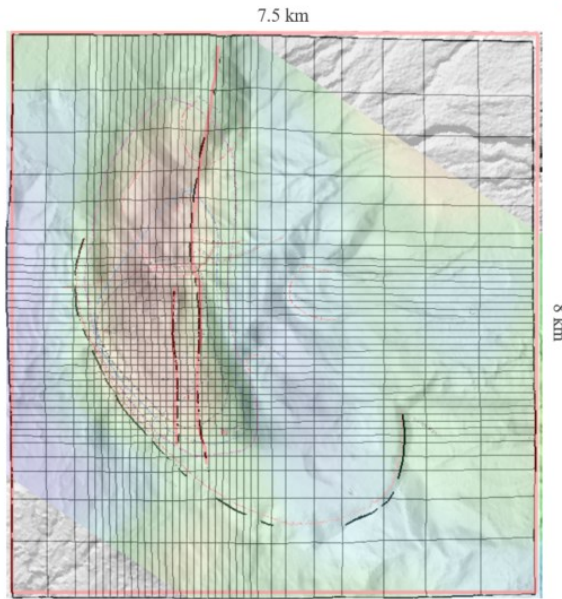


Figure 10: Grid framework of the Sibayak model.

The top most boundary of the model is an atmospheric layer with a pressure of 1 bara and a temperature of 25°C in a fixed state condition. The side boundaries were assumed to be closed by inputting low permeability values (Figure 11). Extra cells with a constant pressure of 215 bara and a temperature of 318°C were added to the bottom of the model acting as a heat source connected to the bottom layers of the model.

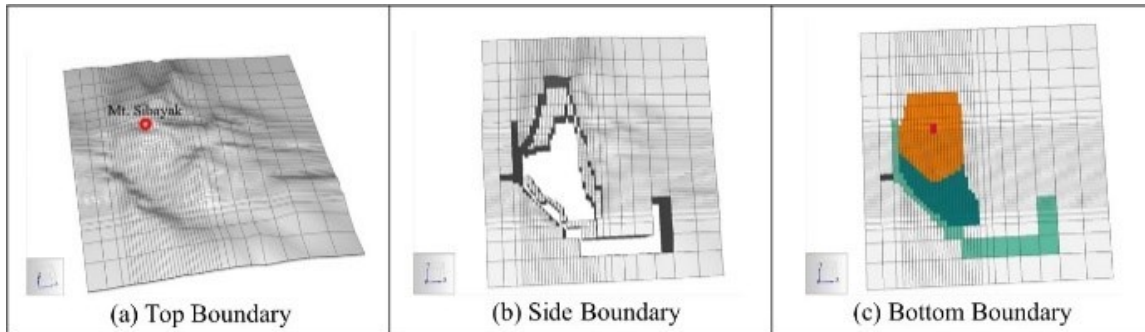


Figure 11: Three boundary shapes: the top boundary with atmospheric condition (a); the side boundary with no-flow condition (b); and the bottom boundary with natural deep upflow conditions at the heat source (c).

More rock properties such as fault, base, heat, caldera, and direction of flow were added to the previous model, in which several properties such as permeability had to be changed by a trial-and-error approach until a steady-state condition with stable pressures and temperatures was obtained. The final rock properties for the model can be seen in Table 1.

Table 1: Final rock properties used in model to obtain a well-matched natural, steady state model.

Rock Type	Rock Density (kg/m ³)	Porosity (%)	Kx (md)	Ky (md)	Kz (md)	Conductivity (W/(m.K))	Specific Heat (kg.K)
ATM	2600	99	100	100	100	2	1000
GW	2600	10	0.4	0.4	0.2	2	1000
CAPR	2600	9	0.004	0.004	0.002	2	1000
FAULT	2600	9	20	50	20	2	1000
BASE	2600	9	0.2	0.2	0.2	2	1000
HEAT	2600	9	20	20	60	2	1000
CALDR	2600	9	0.04	0.04	0.02	2	1000
RES1	2600	9	40	40	20	2	1000
RES2	2600	9	8	8	4	2	1000
FAULT2	2600	9	20	20	10	2	1000
BONDS	2600	9	0.02	0.02	0.02	2	1000
TRAN2	2600	9	8	8	4	2	1000
VULCN	2600	9	0.2	0.2	0.2	2	1000
UPFLW	2600	9	20	20	60	2	1000
TRANS	2600	9	10	10	5	2	1000
BARR	2600	7	0.01	0.01	0.01	2	1000
COLD1	2600	9	1	1	1	2	1000
VERTL	2600	9	0.1	0.1	5	2	1000
LATRL	2600	9	1	1	1	2	1000
VER2	2600	9	0.1	0.1	5	2	1000
LAT2	2600	9	4	4	1	2	1000

The caprock material is indicated by the brown color, while the main reservoir materials are depicted in blue (RES1), purple (RES2), green (UPFLW) in the vertical cross-section shown in Figure 12:

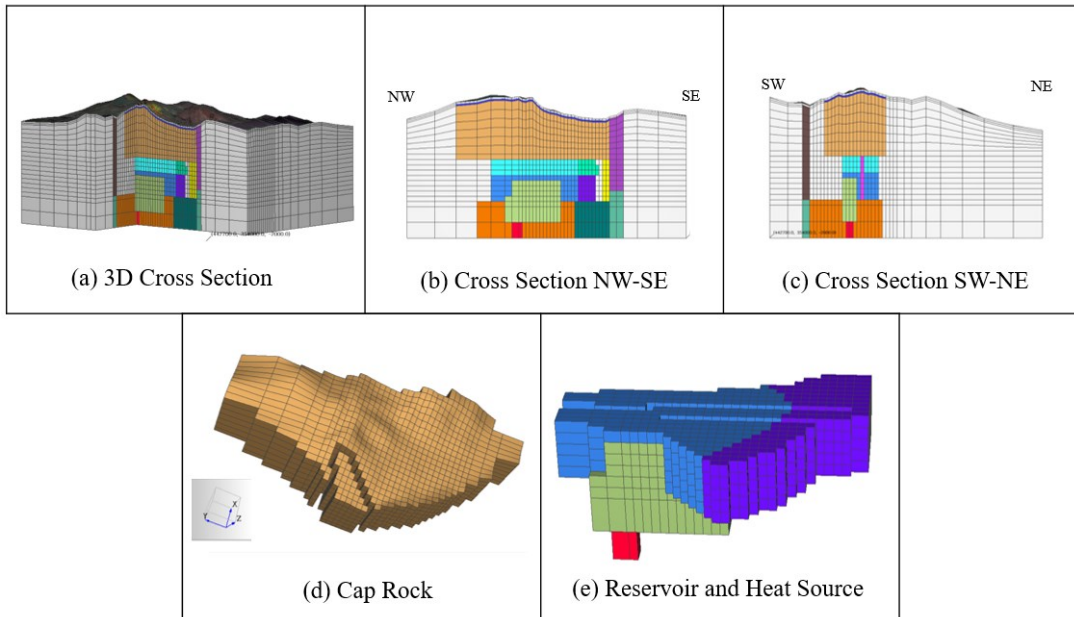


Figure 12: Vertical cross-sections of the material distributions and configuration of the cap rock, reservoir and heat source (a,b,c,d,e).

The visualization of rock types in a horizontal cross-section is shown in Figure 13, with the Injectivity Index (II) from each well converted into Productivity Index (PI). Subsequently from these values, the transmissivity (kh) is calculated to obtain a permeability value within the range of 2-60 mD.

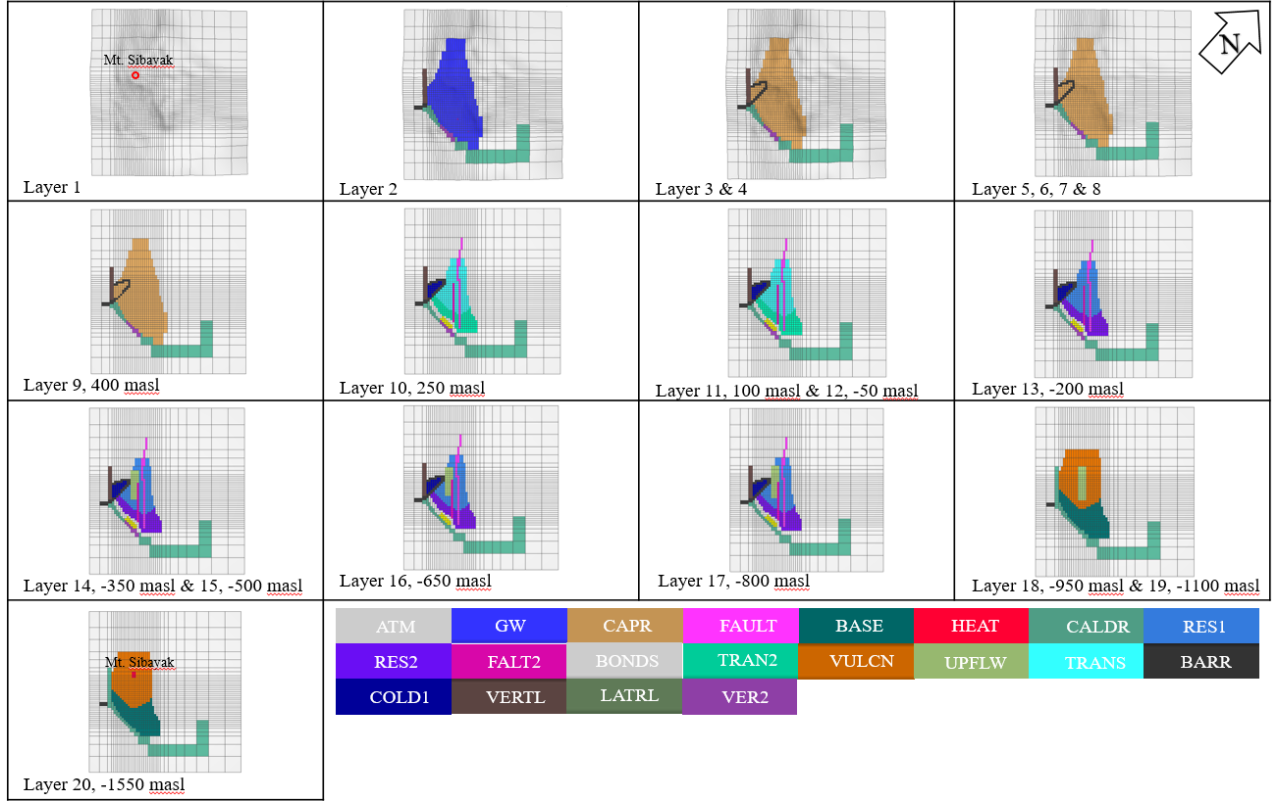
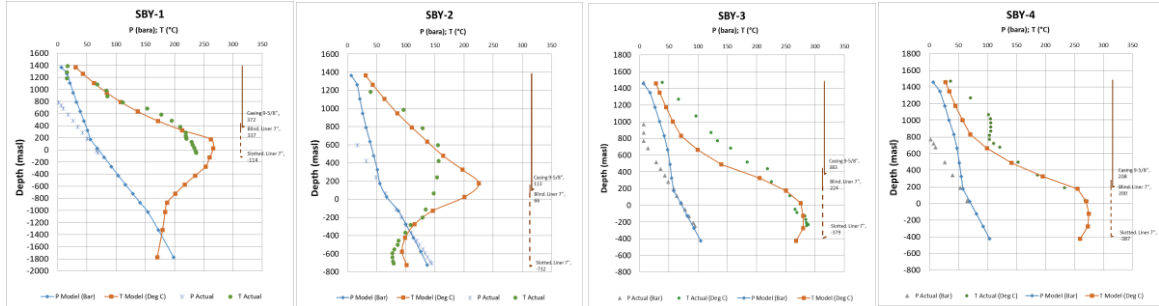


Figure 13: Horizontal slices of materials distribution for each layer.

5. RESULT AND DISCUSSION

In the previous model, only SBY-1, SBY-2 and SBY-6 were used in PT matchings. However in this newly update model, all wells are used for pressure-temperature matchings. The natural state was then run for 3.16×10^{12} s. In Figure 14, pressure-temperature profiles simulated from the model and actual measured data for each well are presented. The simulated profiles generally exhibit a reasonably good match towards the actual data, although some wells show a less significant alignment. Wells that have achieved a satisfactory match include SBY-3, SBY-4, SBY-6, SBY-7, SBY-8, and SBY-9. Despite a few mismatches in a few wells, these wells still demonstrate a consistent temperature trend especially within the reservoir zone. Furthermore, temperatures that deviate from the model are mostly found in the cap rock and above. This is not a significant concern as the creation of the natural state focus more on the reservoir zone.



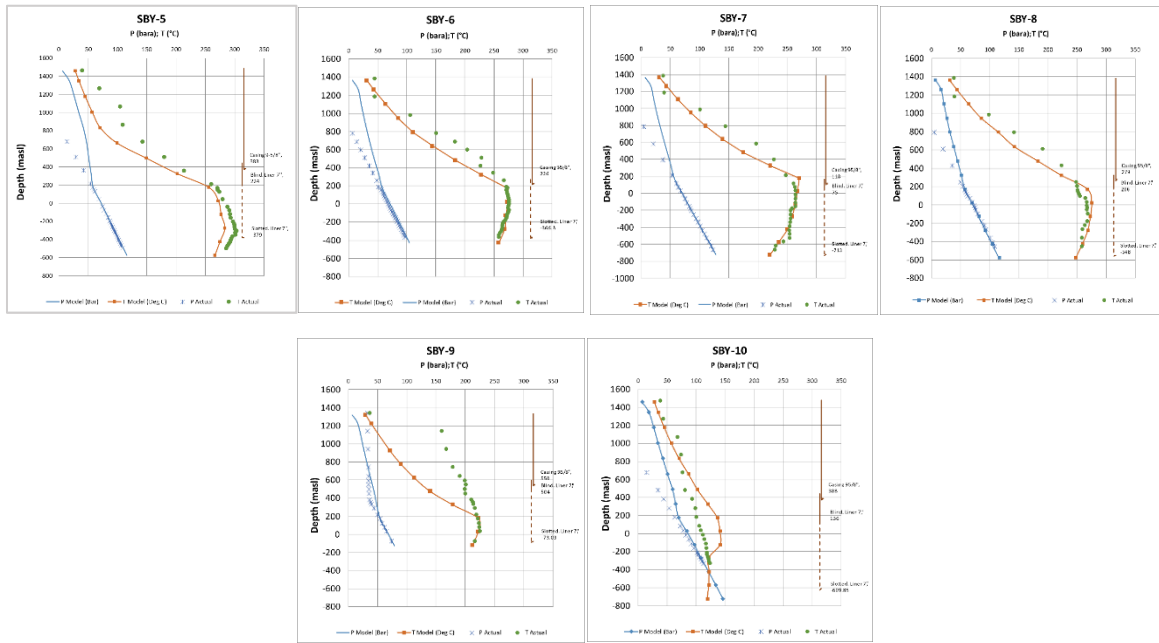


Figure 14: Simulated pressure-temperature profiles matched with field-measured pressure-temperature profiles.

From the natural state model, the temperature distribution in the Sibayak field forms a tongue-shaped pattern pointing southeast, indicating that this area represents an outflow zone. Meanwhile, in the up flow region, heat flows vertically upward from a heat source located beneath Mount Sibayak. This outcome is clearly evident in the vertical cross-section shown in Figure 15. The natural state model thus has represented the updated conceptual model.

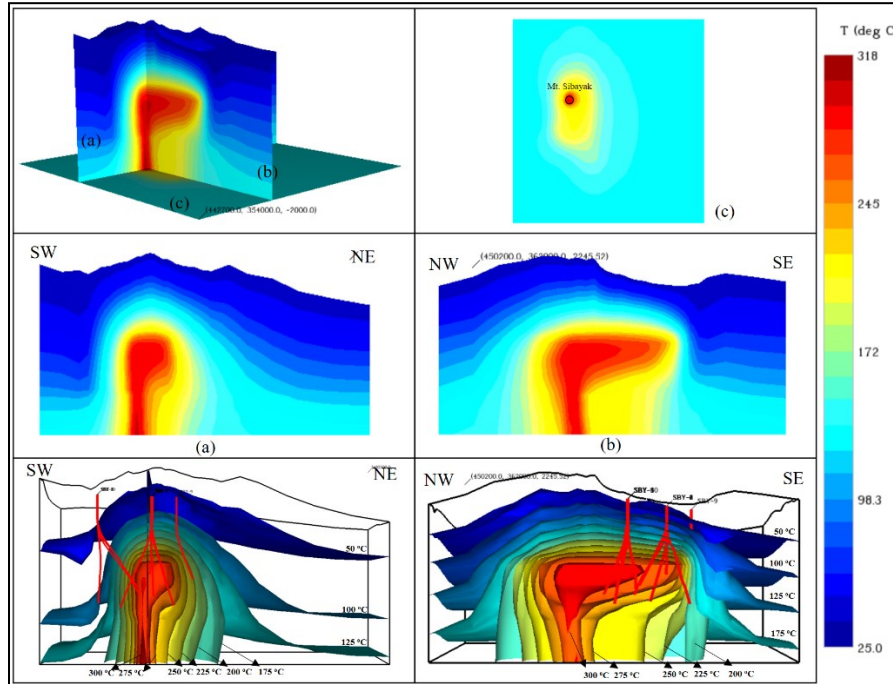


Figure 15: Vertical cross-sections of the temperature distributions.

It can also be seen that hotter temperatures in the Mount Sibayak area are also illustrated in the horizontal cross-section shown in Figure 16. This model indicates that the hottest temperature is observed in the well SBY-5 which is closest to and has a wellpath heading towards Mount Sibayak.

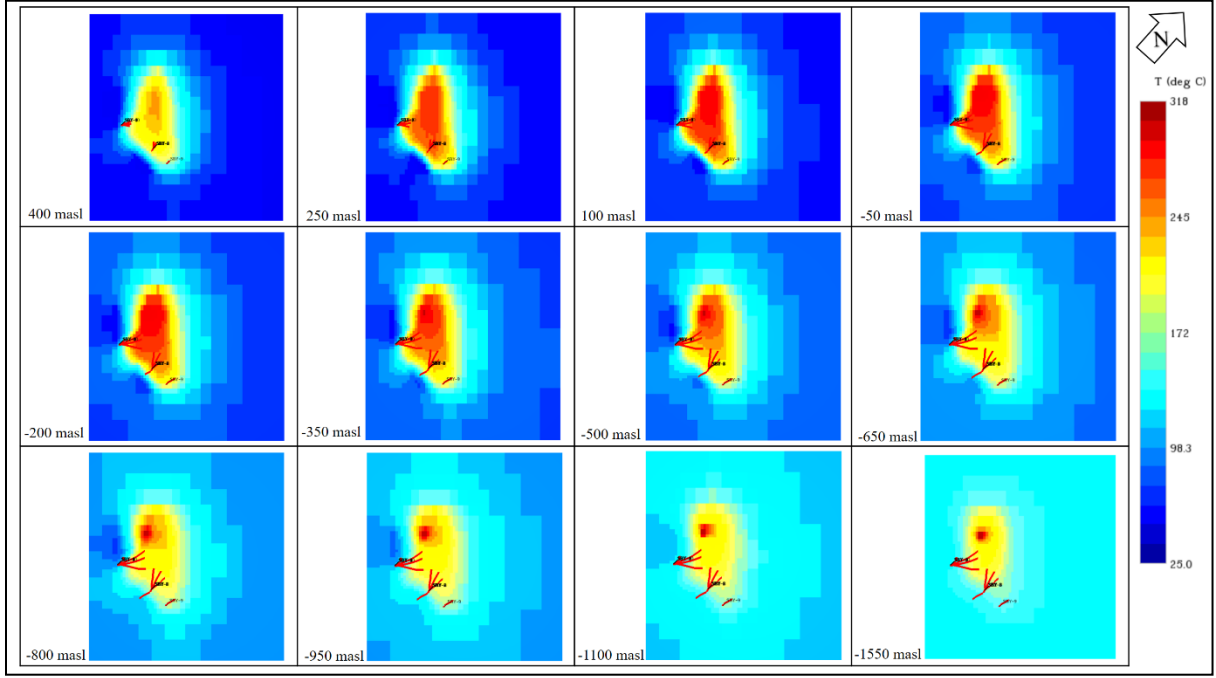


Figure 16: Horizontal cross-sections of the temperature distribution.

The distribution of both upflow and outflow heat as well as the presence of fluid recharge are depicted in Figure 17. In SBY 2, it is apparent that there is an influence of the entry of cold water from the surface towards the lower part of the reservoir, consequently cooling the temperature of SBY-2 and is representative to the isotherms of the new conceptual model. This fluid recharge enters from the surface into the reservoir through the Singkut caldera.

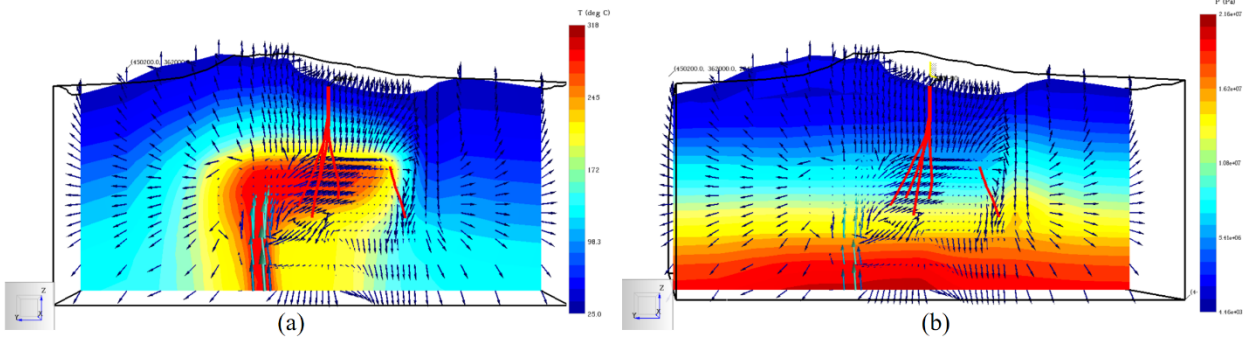


Figure 17: Distribution of heat flow from the heat source (a) temperature; (b) pressure.

6. CONCLUSION

The model generated has represented the reservoir behavior and the geothermal system of the field, in where upflow of Sibayak is located beneath the Mount Sibayak and the outflow flowing to southeast. High temperature profiles are seen to taper out and deflect inwards in deeper depths as the flow goes further out to the southeast, showing recharge areas through caldera faults. Several wells, such as SBY-2, show cooler temperature indicating location of well not located in the main reservoir. Furthermore, this well is likely to be affected by cold water flowing from the surface which then enters through the Singkut caldera. Simulated pressure temperature profiles are well matched with measured pressure temperatures in all of the wells in the field, hence indicating the generated model being a good representative of how the reservoir behaves. The simulated model has also confirmed the updated conceptual model. This model can thus be further used in forecasting the field performance, manage reservoir and reinjection in sustaining the field, as well as plans for future field development.

7. ACKNOWLEDGEMENT

We would like to express our deepest gratitude to PT. Pertamina Geothermal Energy Tbk for their utmost support and permission to publish this paper.

8. REFERENCES

Atmojo, J., Itoi, R., Fukuda, M., Tanaka, T., Daud, Y. and Sudarman, S.: Numerical Modeling Study of Sibayak Geothermal Reservoir, North Sumatra, Indonesia, Twenty-Sixth Workshop on Geothermal Reservoir Engineering, Stanford, California (2001).

Atmojo, J., Itoi, R., Tanaka, T., Fukuda, M., Sudarman, S. and Widiyarso, A.: Modeling Studies of Sibayak Geothermal Reservoir, Northern Sumatra, Indonesia, Proceedings World Geothermal Congress, Kyushu, Japan (2000), 2037-2043.

Daud, Y., Sudarman, S. and Ushijima, K.: Imaging Reservoir Permeability of The Sibayak Geothermal Field, Indonesia Using Geophysical Measurements, Twenty-Sixth Workshop on Geothermal Reservoir Engineering, Stanford, California (2001).

Hochstein, Manfred, P., and Sudarman, S.: Indonesian Volcanic Geothermal Systems, Proceedings World Geothermal Congress, (2015).

PT Dizamatra Powerindo.: Project Conceptual Design Technical Report, Indonesia (1997).

PT Pertamina Geothermal Energy Tbk.: Internal Report: Geological, Geochemistry, Geophysical and Reservoir Evaluation of Sibayak Geothermal Field, North Sumatra, Resource Management Division of Planning and Development Directorate, Jakarta, Indonesia (2016).

PT Pertamina Geothermal Energy Tbk.: Internal Report: Geological Mapping Report of Sibayak Area, Geoscience Region I Exploration Division of Exploration and Development Directorate, Jakarta, Indonesia (2022).

PT Pertamina Geothermal Energy Tbk.: Internal Report: Reservoir Re-Assessment of Kamojang, Lahendong, and Sibayak Area (Part Three: Sibayak Area), Jakarta, Indonesia (2008).

PT Pertamina Geothermal Energy Tbk.: Internal Report: Reservoir Assessment and Development Feasibility and Natural State Modelling of The Sibayak Geothermal Field, Geothermal Division of Exploration and Production Directorate, Jakarta, Indonesia (1994).